Velocity, Depth-of-Cut, and Physical Property Effects on Saw Chain Cutting

Andrew Otto and John Parmigiani*

A better understanding of saw-chain cutting mechanics is needed for more efficient chainsaw designs. The effects of varying key parameters such as workpiece moisture content, workpiece density, cutting velocity, and depth-of-cut, while established for other types of cutting, are largely unexplored and/or unpublished for saw chains. This study contributes to filling this gap through experimentation and analysis. Experiments were conducted using a custom-built saw-chain testing apparatus to measure relevant forces over a range of workpiece moisture contents, workpiece densities, cutting velocities, and depths-of-cut. Analysis consisted of fitting linear regression models to experimental data, identifying trends, and exploring optimum cutting conditions. Results showed that over the range of values included in the study, workpiece moisture content and density had effects that depended on the depth-of-cut. Cutting velocity had a small effect, and depth-of-cut had a large effect. All trends fit well with linear models; however, depth-of-cut required one linear fit for small-to-mid values and a second fit for mid-to-large values. Maximum efficiency was found to occur at a depth-of-cut equal to the transitional value between fits. These results provide basic relationships that can lead to the more effective and efficient use and design of chainsaws.

Keywords: Chainsaw; Saw chain; Cutting forces; Cutting efficiency; Linear regression

*Contact information: Department of Mechanical, Industrial, and Manufacturing Engineering, Oregon State University, 204 Rogers Hall, Corvallis, OR 97331 USA; *Corresponding author: parmigjo@engr.orst.edu*

NOMENCLATURE

F	Force magnitude [N]
F_C	Cutting force [N]
F_{CH}	Chain force [N]
F_F	Feed Force [N]
F_T	Chain tension [N]
k	Shear yield strength [N/m^2]
L	Length of cut [mm]
MC	Workpiece moisture content [%]
n	Number of drive sprocket teeth
P	Saw chain pitch [mm]
Q	A function of friction coefficients and tool geometry [dimensionless]
R	Specific work of surface separation [J/m^2]
S	Saw chain tooth spacing
T_M	Drive-sprocket torque [N m]
V_C	Cutting velocity [m/s]
V_F	Feed velocity [m/s]
w	Kerf width [m]

β_i Regression model coefficients [varies]
δ Depth of cut [mm]
δ_{DG} Saw chain depth gauge setting [mm]
δ_{OL} Overload depth-of-cut [mm]
ΔF Change in force magnitude [N]
ΔPV Change in the varying predictor variable [varies]
γ Shear yield strain [dimensionless]
η Cutting efficiency [mm^2/J]
ρ Workpiece density [kg/m^3]
ω Drive-sprocket angular velocity [radians/s]

Throughout the text, a symbol with an over-bar (*e.g.* $\bar{x}$) denotes a mean value, and a symbol with an asterisk superscript (*e.g.* x^*) denotes a value less its mean value (*i.e.* $x^* = x - \bar{x}$)

INTRODUCTION

Whether harvesting forest trees, performing storm cleanup, clearing trees, or mitigating wildfires, a chainsaw is a common tool for cutting wood. Increased efficiency and effectiveness are highly desired by both professional and home users. In particular, chainsaw manufacturers are interested in increasing energy efficiency for cordless electric chain saws in order to maximize operating performance and duration due to the relatively low power density of batteries. Designing chainsaws to meet these needs requires an understanding of chainsaw cutting mechanics, which typically involves experimentation. This is complicated by variations in the physical properties (*e.g.*, density) of the wood workpieces used in testing. Two important aspects of saw chain cutting mechanics are the roles of chain velocity and depth-of-cut. Changes in chain velocity and depth-of-cut can affect cutting forces and thus affect energy consumption and efficiency. Significant published research exists regarding the effects of wood specimen variability, cutting velocity, and depth-of-cut, but most studies have involved orthogonal cutting and rigid-cutter sawing (*i.e.*, sawing in which individual cutter teeth do not move relative to each other, as in band saw blades and circular saw blades but not saw chains). Thus, a significant gap in understanding exists regarding these effects in saw chain cutting.

Workpiece physical properties play a large role in woodcutting. As a natural material, wood exhibits a high degree of variation that complicates the effect of material properties on cutting. Studies in orthogonal cutting and rigid-cutter sawing have shown that cutting forces increase with density and decrease with moisture content up to the fiber saturation point (Kivimaa 1950; Franz 1958; Koch 1964). However, moisture content and density alone are inadequate predictors of cutting force. The orthogonal cutting and rigid-cutter sawing of different species with the same moisture content and density will generally result in different cutting forces (Franz 1958; Koch 1964; Cristovao *et al.* 2012). More recent research has made use of other physical properties to describe the influence of the work piece on cutting forces. Naylor *et al.* (2012) successfully formed a species-independent linear regression model of cutting forces for rigid-cutter sawing using material strength and fracture toughness. However, the authors know of no published work specifically for saw chain that quantifies the effect of physical properties on cutting forces.

A significant body of research exists regarding the effect of cutter velocity in woodcutting. In orthogonal cutting, it is widely accepted that cutting velocity has little to no impact on cutting forces (Kivimaa 1950; Franz 1958; McKenzie 1961). However, in the area of rigid-cutter sawing, Koch (1964) suggests several effects that can cause cutting forces to become velocity-dependent—acceleration of chips out of the saw kerf, strain rate-dependent failure of wood, and changes in frictional behavior between the tool and work piece at varying velocities. Also in the area of rigid-cutter sawing, Orlowski *et al.* (2013) found that chip acceleration must be accounted for in the characteristically higher speeds of band sawing and circular sawing to accurately predict power requirements, suggesting that cutting velocity influences cutting forces at high speeds. Regarding saw chains, Stacke (1989) developed a fully dynamic model for the motion paths of saw chain cutters within the kerf and illustrated the influence of chain velocity and inertia on the saw chain cutting process. His findings suggest that chain momentum acts to smooth the motion path of a cutter, reducing cutting forces and energy consumption. Additionally, Stacke showed that higher chain velocities increase the drive torque on a free running chain due to chain-bar friction, reducing cutting efficiency. Heinzelmann *et al.* (2011) also states that frictional losses in the chainsaw cutting system increase with chain velocity, and therefore claims that achieving reasonable battery life for battery-powered applications requires the chain to run at lower speeds than those typical of gasoline-powered saws. However, this research does not conclusively establish that reduced cutting velocity will improve overall cutting efficiency. For example, research has not been conducted to determine whether the reduced frictional losses occurring at low cutting velocities will translate into overall gains in chainsaw efficiency or if they will be offset by the rough-cutting inefficiency of a slow-moving, low-momentum saw chain. The authors found no published literature defining an optimum cutting velocity for saw chain.

Research on the effect of depth-of-cut exists for orthogonal cutting, rigid-cutter sawing, and, to a lesser extent, for saw chain cutting. For both orthogonal cutting and rigid-cutter sawing under typical operating conditions, a linear relationship between cutting force and depth-of-cut has been shown to work well by a number of researchers (Kivimaa 1950; Franz 1958; McMillin and Lubkin 1959; McKenzie 1961; Koch 1964; Gronlund 1988; Bucar and Bucar 2002; Atkins 2009; Wyeth *et al.* 2009). Under non-typical rigid-cutter sawing conditions, when excessive depths of cut are used, cutting forces and energy consumption have been found to increase in a non-linear fashion (Koch 1964). This non-linear behavior is loosely correlated with the effects of chip transport and cutter geometry, but lacks experimental data for confirmation. Also in the area of rigid-cutter sawing, Oehrli (1960) reported an optimal value of depth-of-cut with respect to energy consumption for a circular saw. Little research has been conducted on the effect of depth-of-cut for saw chain. It has been found that when depth-of-cut roughly equals the depth gauge, sliding friction between the saw chain and wood increases greatly (McKenzie 1955). Regression models based on experimental data have shown that cutting forces increase with increasing depth-of-cut (Reynolds *et al.* 1970). Also, it has been determined that cutting rates increase dramatically when the depth gauge setting is enlarged (Coutermarsh 1989). However, no published literature has been found that defines the relationship between depth-of-cut and cutting efficiency for saw chain or for identifying an optimum depth-of-cut.

The work presented in this paper considers the effects of workpiece moisture content, workpiece density, cutting velocity, and depth-of-cut on saw-chain cutting forces and saw-chain cutting efficiency. Moisture content and density were measured for each offcut. Cutting velocity and depth-of-cut were specified over a range appropriate for a

battery-powered electric chain saw. Cutting forces were measured using a test apparatus constructed by the authors specifically for saw chain. Key aspects of this paper include effectively modeling the effects of moisture content, workpiece density, cutting velocity, and depth-of-cut on cutting forces using a multiple linear regression model, using this model to demonstrate trends in cutting forces and cutting efficiency, and identifying conditions corresponding to optimum cutting efficiency.

EXPERIMENTAL

Terminology

The cutting parameters that were measured in this study are illustrated in Fig. 1, a schematic of a chainsaw cutting a workpiece. The cutting force (F_C) and the feed force (F_F) are the components of the reaction force acting on the workpiece in directions parallel to the guide bar and normal to the guide bar, respectively. Torque (T_M) is the input torque applied to the drive sprocket to propel the saw chain, and ω is the angular velocity of the drive sprocket. The force (F_T) is the non-cutting chain tension (*i.e.*, chain not in contact with the workpiece). The feed velocity (V_F) is the velocity of the guide bar into the cut (*i.e.*, normal to the guide bar for the cuts performed in this work).

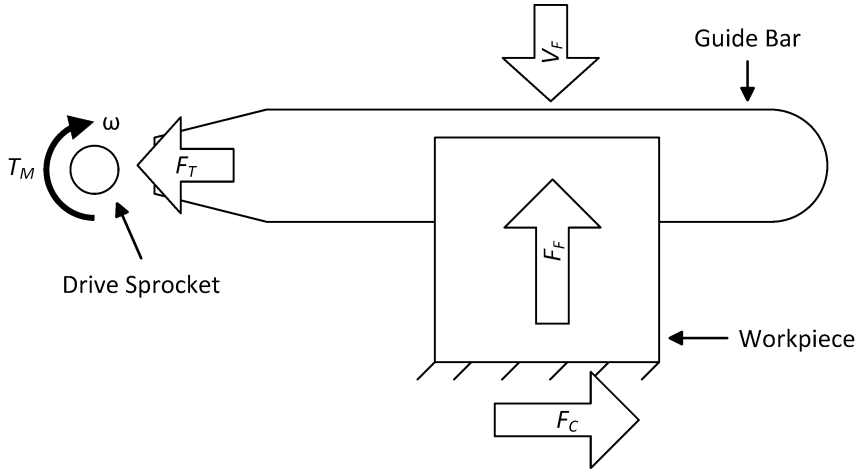

Fig. 1. A schematic of a chainsaw cutting a workpiece showing the measured cutting parameters of drive torque and velocity, chain tension, feed force and velocity, and cutting force

Saw chain terminology is illustrated in Fig. 2 for a typical saw chain as used in this study. This saw chain consists of three types of links connected by rivets: drive links, cutter links, and tie straps. Drive links engage the drive sprocket to propel the chain and also slide through a notch in the guide bar to constrain the saw chain to move about the guide bar periphery. Cutter links consist of a cutter tooth and a depth gauge. Cutter teeth curl above the cutter-link body and alternate in orientation between teeth pointing to the left and pointing to the right. The cutter teeth perform the actual cutting by removing a chip from the work piece. The depth gauge limits the thickness of the cut chip. Tie straps connect drive links and cutter links. The distance between the top of the depth gauge and the sharp edge of the cutter tooth is the depth gauge setting (δ_{DG}). Tooth spacing (S) is defined as the number of rivets between cutter teeth of the same orientation and is equal to eight for a

standard sequence chain. Chain pitch (P) is defined as half the distance between the end of a cutter link and the corresponding end of an adjacent tie strap.

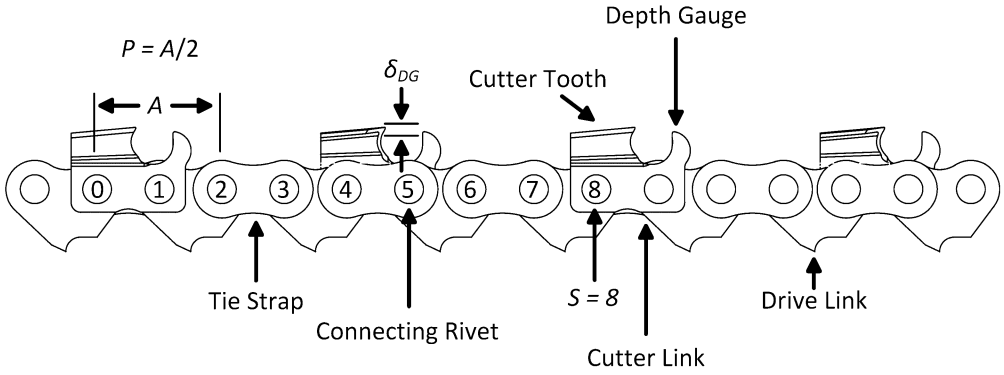

Fig. 2. Saw chain terminology

The parameters defined above were used to calculate the three quantities listed in Table 1. The chain force (F_{CH}), given by Eq. 1, is the cutting chain tension (*i.e.*, the force applied to the chain by the drive sprocket during cutting). It can be calculated from the drive sprocket torque, the chain pitch, and the number of sprocket teeth (n). The cutting velocity (V_C), given by Eq. 2, is the velocity of the moving saw chain and can be calculated from the sprocket angular velocity, the chain pitch, and the number of teeth on the sprocket. The depth-of-cut (δ), given by Eq. 3, is the average thickness of a chip removed by an individual cutter tooth and can be calculated from the chain velocity, feed velocity, chain pitch, and tooth spacing. Note the depth gauge of the saw chain only acts to inhibit depth-of-cut greater that the depth gauge setting and does not independently determine depth-of-cut.

Table 1. Calculated Cutting Parameters, Equations 1 through 3

Parameter	Calculation	
Chain Force [N]	$F_{CH} = \frac{\pi T_M}{1000 Pn}$	(1)
Chain Velocity [m/s]	$V_C = \frac{1000 Pn\omega}{\pi}$	(2)
Depth-of-cut [mm]	$\delta = \frac{V_F}{V_C} P S$	(3)

Test Apparatus

A test apparatus was designed and built for this study. The apparatus consists of four components: a power head, a motion system, a work holding system, and a data acquisition system. The three mechanical components are shown in Fig. 3.

The power head, illustrated in Fig. 4, propels the saw chain and measures several test parameters. A 1.5-kW AC motor was used, corresponding to the power typically available for smaller gasoline-powered and electric battery-powered saws. The motor is capable of speeds up to 7,000 RPM and is controlled through a variable frequency drive.

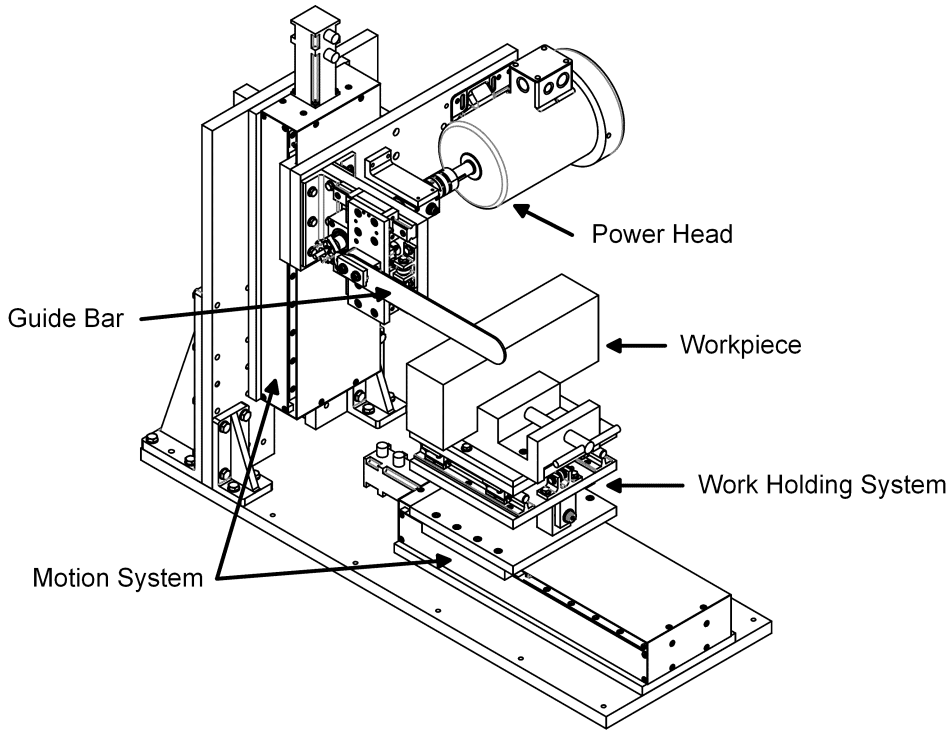

Fig. 3. Mechanical components of the saw chain test apparatus

The guide bar is mounted to linear bearings whose motion is opposed by a load cell (670 N measuring range) that measures chain tension. Standard commercial guide bars and chains can be used. Lubricating oil for the saw chain is provided in the same manner as a typical commercial chainsaw, through the orifice on the guide bar. Chain tension is adjusted with the screw system common to typical commercial chainsaws. An inline torque transducer (20 N m measuring range) with optical encoder, located between the motor and the drive sprocket, measures input torque and drive sprocket angular velocity.

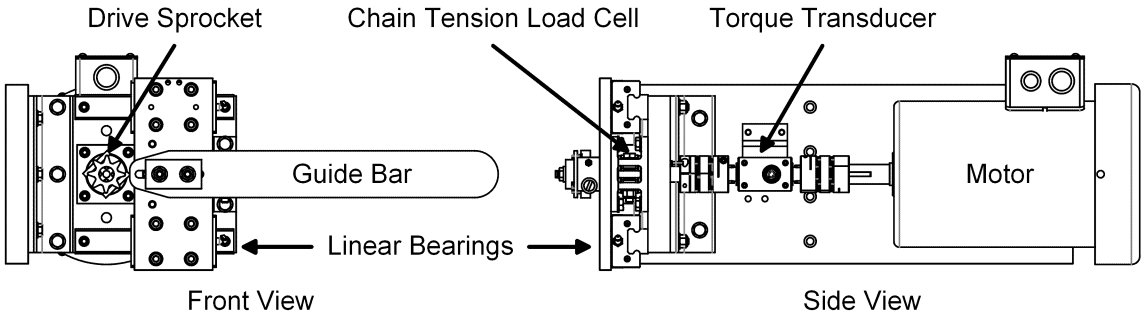

Fig. 4. Test apparatus power head

The work holding system, shown in Fig. 5, holds the workpiece and measures the cutting force and feed force. A drill-press vise is used to hold the workpiece. The cutting force is measured using a linear bearing system opposed by an S-beam load cell (1300 N measuring range), similar to that of the chain-tension measurement system on the power head. The feed force is measured using a pivot mechanism and S-beam load cell (450 N measuring range).

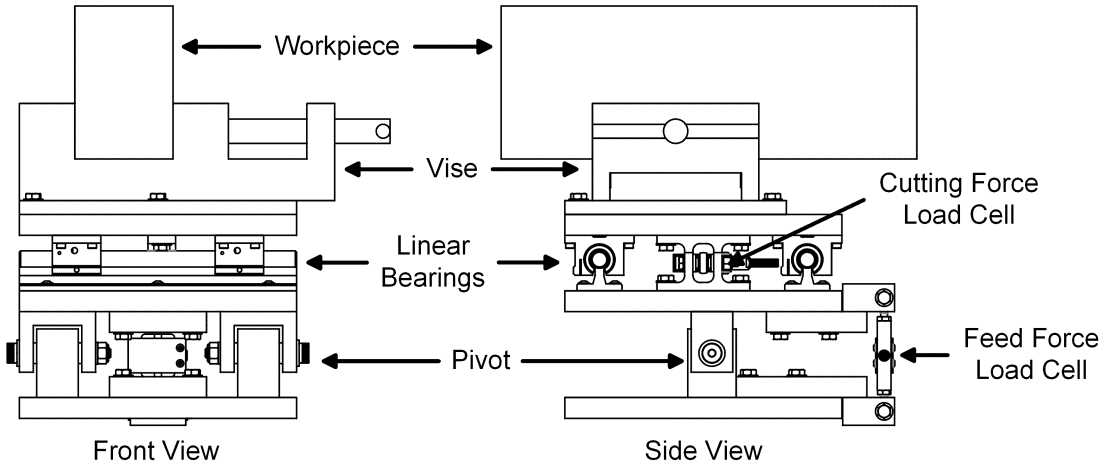

Fig. 5. Test apparatus work holding system

The motion system is comprised of two identical linear motion slide tables. These tables move vertically and horizontally relative to, and in the plane of, the bar and have a maximum linear speed of 83 mm/s. They are driven by a 400 Watt servo motor. The vertical slide table provides the mounting surface for the power head. An incremental optical encoder is used for feedback control and measurement of feed velocity. The horizontal axis provides the mounting surface for the work holding system.

The data acquisition system records all measurements and saves the output to disk after each cut. Machine control and data acquisition are accomplished using a National Instruments (USA) Compact RIO programmable automation controller. Force channels are sampled at 2 kHz and filtered using a 200 point moving average filter. A personal computer with LabVIEW (National Instruments) provides the user interface to the machine.

Materials

Workpieces for all testing were obtained from Douglas-fir dimensional timbers. Each timber had a rectangular cross-section (90 mm by 140 mm), a length of 3.0 m, and was purchased from a local supplier. Four timbers were used, denoted A through D in Fig. 6, and each was cut into four 0.75-m workpieces, sized to fit inside the safety enclosure of the test apparatus.

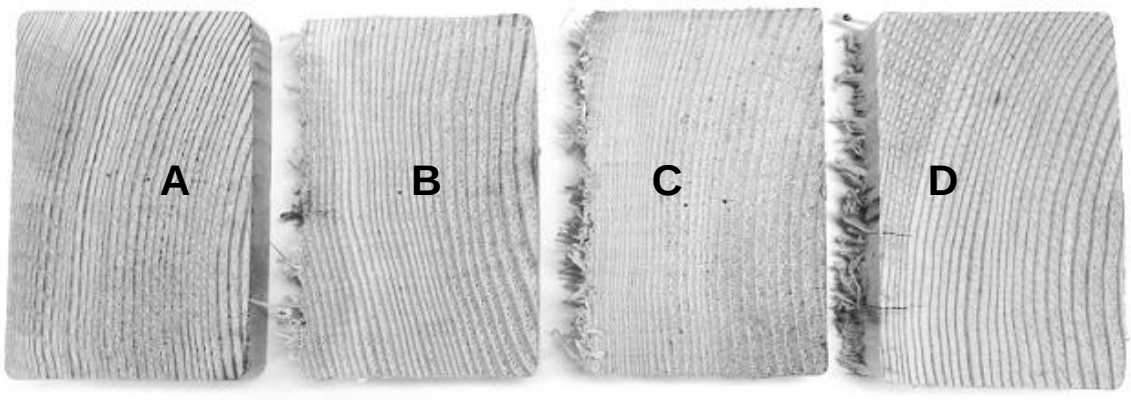

Fig. 6. Grain orientations of the four timbers (A–D) used in testing

Each timber had roughly similar grain orientations with growth rings oriented vertically so that cuts were made perpendicular to the rings, thus passing through equal amounts of early and late wood. During testing, cuts on each 0.75-m workpiece were separated by 25 mm, giving a total of 20 offcuts per workpiece. Immediately following cutting, each offcut was labeled with an identification number for the purpose of visual inspection and to track the occurrence of knots.

Test Procedure

Each use of the test apparatus to complete a cut and collect data followed the same procedure. First, the guide bar and saw chain were installed on the power head. Next, the workpiece was oriented as shown in Fig. 6 and secured in the vice of the work holding system such that the cut would occur at the desired location. Then the drive sprocket rotational velocity and feed velocity, as determined from the desired depth-of-cut and chain velocity using Eqs. 2 and 3, were set. Chain lubricating oil was applied at the desired rate. The non-cutting chain tension was then determined by calculating the average over a 2-second time period of the measured chain tension while the chain was free running (*i.e.*, driven by the drive sprocket rotating at the specified rotational velocity and without making contact with the workpiece). Adjustments to the chain tension, if necessary, were made using the screw adjustment on the power head. The weight of workpiece was measured. The desired feed velocity was then set and the cut was performed. Following cutting, the machine returned to its initial position and data were saved for post processing. Moisture content was measured immediately following each cut using a Delmhorst J-2000 moisture meter by manually inserting the meter's probe into the center of the workpiece cut cross-section. The workpiece density corresponding to a cut was calculated by dividing the mass of the offcut by its volume. Mass was measured using a gram scale. Volume was measured using digital calipers.

Data Processing

Prior to analysis, several data processing steps were performed. Noise was removed from the cutting force data with a 200-point (0.1-second) moving-average filter. The effect of workpiece weight was removed from the feed force by subtracting the weight of the workpiece from the feed force measured during cutting. The increase in measured forces due to knots or other defects in the workpiece was addressed by using the modal value of force rather than the mean value. More specifically, during a cut in defect-free wood, forces remain approximately constant during cutting, and a simple mean value can characterize cutting forces accurately. However, when a knot or highly distorted grain is encountered in the work piece, force magnitudes increase, often significantly. This effect is illustrated in Fig. 7 with representative data for the chain force, cutting force, and feed force.

Because the intent was to study the cutting of wood without including the presence of knots and other defects as an additional variable, this effect needed to be addressed. A simple mean value is not appropriate because it inherently results in force magnitudes above the defect-free values. The alternative method used was to calculate the most frequently occurring force magnitudes (the modal value). This approach is illustrated in Figs. 8 and consisted of defining 15 equally spaced intervals spanning the minimum to maximum instantaneous force values occurring during the cutting period. The midpoint of the interval containing the greatest number of data points is defined as the characteristic force value for that cut. All force values were calculated using this method and all cuts, whether encountering knots or not, were included in the subsequent data analysis.

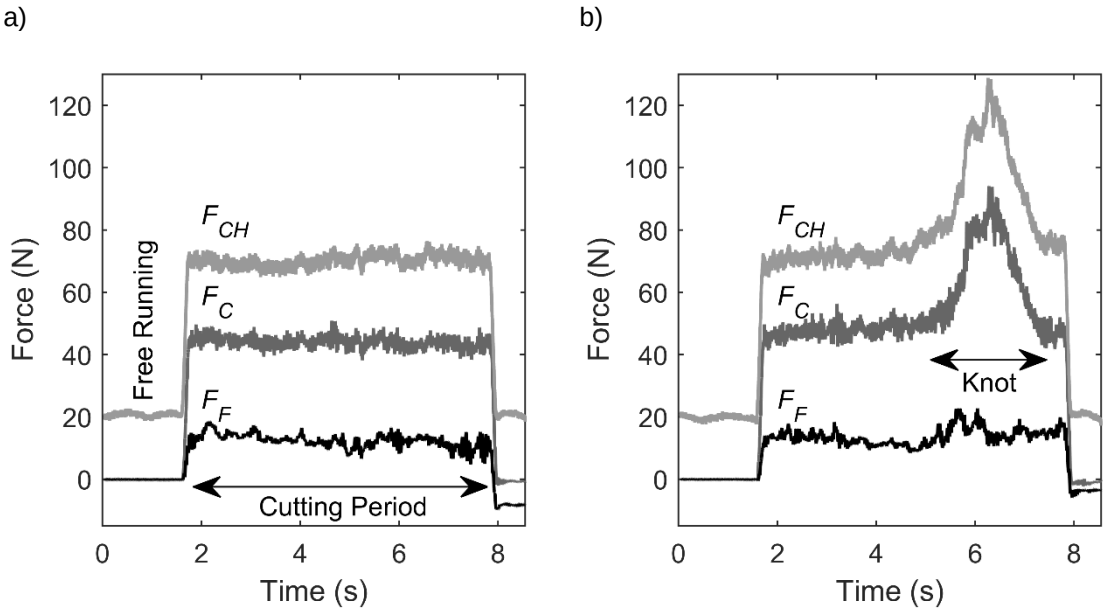

Fig. 7. An example of force magnitudes as functions of time for a single cut in (a) a workpiece without knots or other defects and (b) a workpiece with a knot

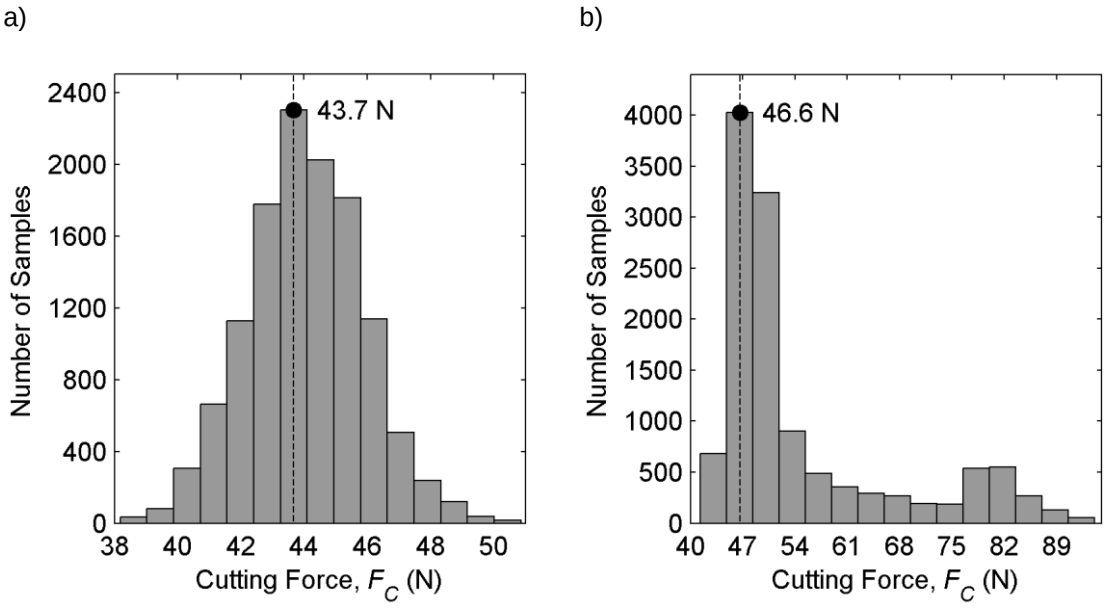

Fig. 8. Histograms, corresponding to the data of Fig. 7, of cutting-force magnitudes showing the number of samples (*i.e.* data points measured during a single cut) in each of 15 equally-spaced intervals for (a) a workpiece without knots or defects and (b) a workpiece containing a knot. The labeled force magnitude is defined as the characteristic force value for the cut.

Data Analysis

The primary data analysis method used was multiple linear regression. The selected response variables were chain force, cutting force, and feed force. Four predictor variables were used for each response variable: the controlled (specified) variables of chain velocity and depth-of-cut and the uncontrolled (measured) variables of workpiece moisture content and workpiece density. For each of the three response variables, all single-factor predictor-

variable main effects and two-factor predictor-variable interaction effects were considered as being possibly significant. Three-factor and higher interaction effects were all assumed to be negligible and were not considered.

RESULTS AND DISCUSSION

Collected Data and Regression Model

Testing consisted of repeated cuts at varying chain velocities and depths-of-cut. Specifically, four chain velocities (3.81, 5.72, 7.62, and 9.52 m/s) and seven depths-of-cut (0.05, 0.15, 0.25, 0.35, 0.45, 0.55, and 0.65 mm) were specified. Each combination of chain velocity and depth-of-cut was repeated eight times for a total of 224 cuts. Workpiece moisture content and density were measured for all offcuts. Two replicates were made within each of the four 3.0 m timbers (A, B, C, and D), and runs were dispersed randomly to reduce systematic error. For all cuts, chain tension was held constant at 89 N (±5 N). Chain lubricating oil was applied at 5 mL/min as recommended by the manufacturer. The chain used had a 9.525-mm (3/8 inch) pitch, a standard sequence, and a depth gauge setting of 0.635 mm. A six-tooth spur sprocket was used. All chains, bars, and sprockets used for testing were in a new, out-of-box condition. The chain was replaced halfway through testing to limit the effect of dulling on cutting force data.

Prior to determining coefficients for the regression models, the collected data were analyzed. The mean and standard deviation of moisture content (*MC*) and density (ρ) are given in Table 2. Overall, moisture content varied from 12.0% to 24.8%, and density from 500 kg/m^3 to 695 kg/m^3. The larger standard deviation in wood density in workpiece C is attributed to a higher occurrence of knots compared with the other three workpieces.

Table 2. Measured Moisture Content and Density

Timber	*MC* (%)		ρ (kg/m^3)	
	Mean	*Standard Deviation*	*Mean*	*Standard Deviation*
A	18.4	1.46	561	23.7
B	17.8	1.28	521	20.4
C	22.7	2.10	556	31.8
D	23.4	0.23	541	16.9
All	20.6	2.86	544	28.4

Chain force, cutting force, and feed force, for each of the 224 cuts performed, is shown *versus* depth-of-cut in Fig. 9. This data shows that the relationship between chain force and depth-of-cut was best described by two linear regions, one extending from small depth-of-cut to a depth-of-cut of approximately 0.45 mm and a second extending from 0.45 mm to a large depth-of-cut. Increased variance in cutting forces at larger depths of cut, as seen in Fig. 9, can be attributed to the increased influence of moisture content and density on the cutting forces at higher depth of cut as well as a reduced ability to maintain cutting velocity near the machine's power limit, thus resulting in reduced ability to maintain constant depth of cut during a single cut. An analysis of force *versus* moisture content, force *versus* density, and force *versus* cutting velocity did not show similar bilinear behavior (*i.e.*, a simple linear fit was sufficient for all parameters except depth-of-cut).

Similar increases in the rate-of-change of force at high depths-of-cut have been observed for saw chain cutting by McKenzie (1955) and can be inferred for rigid-cutter sawing from the work of Koch (1964). However, using a bilinear approach is a new method for modeling this phenomenon.

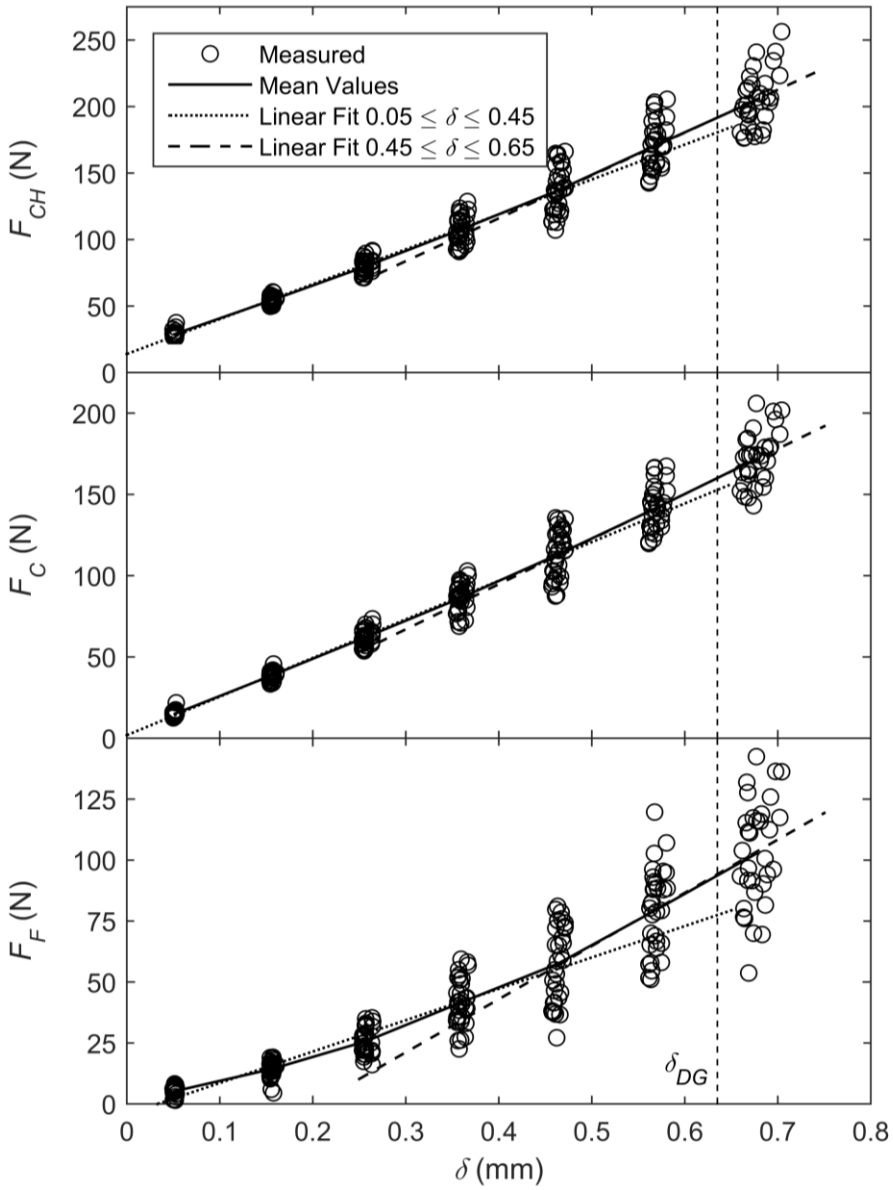

Fig. 9. Measured chain force, cutting force, and feed force *versus* depth-of-cut showing two linear regions

With consideration for the bilinear behavior of the force *versus* depth-of-cut relationship, the regression equations for chain force, cutting force, and feed force were calculated. For each of the three forces, the same eight terms were included: a constant term, main effect terms for moisture content, density, and cutting velocity, two main effect terms for depth-of-cut (the second including the bilinear response), an interaction term for moisture content and depth-of-cut, and an interaction term for density and depth-of-cut. Higher order terms and other interactions were not found to be significant based on their t-

statistic with regressions containing those additional terms. Main effect terms and interaction terms were centered about mean values. Thus, the general form of the regression model is:

$$F_{CH}, F_C, F_F = \beta_0 + \beta_1(MC^*) + \beta_2(\rho^*) + \beta_3({V_C}^*) + \beta_4(\delta^*) + \beta_5\langle\delta - \delta_{OL}\rangle + \beta_6(MC^*)(\delta^*) + \beta_7(\rho^*)(\delta^*), \quad (1)$$

where

$$\langle\delta - \delta_{OL}\rangle = \begin{cases} 0 & \text{if } \delta^* \le \delta_{OL} - \bar{\delta} \\ \delta - \delta_{OL} & \text{if } \delta^* > \delta_{OL} - \bar{\delta} \end{cases}.$$

The β_i factors are the regression model coefficients, over-bars indicate mean values (*e.g.*, $\bar{\delta}$ is the mean value of depth-of-cut for all 224 cuts of the study), the asterisk superscripts refer to the indicated quantity minus its mean value (*e.g.*, $MC^* = MC - \overline{MC}$), and δ_{OL}, referred to as the overload depth-of-cut, is the depth-of-cut corresponding to the transition in the bilinear force response. Its value was calculated to provide the best fit for all three forces. The increase in force at high depths-of-cut is provided by the expression in Macaulay brackets $\langle\delta - \delta_{OL}\rangle$.

The regression model coefficients, mean values, overload depth-of-cut, and fit parameters are given in Table 3. The regression model provided excellent fits for each of the three forces. The R^2 values were all above 0.9, indicating that the regression models capture variance in the data very well. The F-statistic for each model was well above the critical value required for significance ($F_{7,216,.01}$ = 2.707) and also passes the "4-to1" rule that states the F value be at least 4 times larger than the critical value (Ryan 2009).

Table 3. Regression Coefficients, Parameters, and Fit to Data

	Regression Coefficients								Fit	
	β_0	β_1	β_2	β_3	β_4	β_5	β_6	β_7	R^2	F
F_{CH}	109.56	−2.39	0.16	−0.62	264.83	62.77	−8.30	0.31	0.98	1470
F_C	88.24	−2.20	0.15	−0.65	238.61	41.02	−6.68	0.30	0.99	2440
F_F	43.03	−1.75	0.15	−0.33	131.68	98.63	−6.59	0.37	0.91	323
Predictor Variable			***MC***		***ρ***		***V_C***		***δ***	
Mean Value			20.57 %		544.8 kg/m^3		6.51 m/s		0.362 mm	
δ_{OL} **= 0.5 mm**										

Several significant data trends can be identified from an inspection of the regression coefficients. The signs of each coefficient and the approximate magnitudes of each coefficient were the same for each of the three response variables (forces). This indicates that the general response of each of the three forces to changes in the predictor variables was the same. Specifically, the coefficients for the moisture content and the cutting velocity main effects were negative, indicating that forces tended to decrease with increasing moisture content and cutting velocity. However, the coefficient for the density and depth-of-cut main effects were positive, indicating the reverse (forces tend to increase with increasing density and depth of cut).

Effect of Predictor Variables on Response Forces

To demonstrate relative and interaction effects of the predictor variables on the response variables, three cases were defined for use with the regression model and denoted

as *mid-force*, *high-force*, and *low-force*. Each of the three cases was applied to each of the four predictor variables, one at a time. Applying the mid-force case to a predictor variable consisted of varying it from a low value to a high value and holding the other three predictor variables constant at their mean value. When moisture content was the varying predictor variable, it was varied from a low value of its mean minus one standard deviation to a high value of its mean plus one standard deviation. When density was the varying predictor variable, its range was similar with a low value of its mean minus one standard deviation and a high value of its mean plus one standard deviation. Cutting velocity, being a controlled variable, was varied differently with a low value of the nominal minimum value included in the study (3.81 m/s) and a high value of the maximum value included in the study (9.525 m/s). Depth-of-cut was varied similarly, from its minimum nominal value (0.05 mm) to its maximum nominal value (0.65 mm).

The second case, the high-force case, also consisted of varying one of the predictor variables between the same low and high values and holding the other three predictor variables constant. However, instead of being held constant at their mean values, they were held constant at either their low value or high value depending on which increased the value of the response variable above the mid-force value. For example, when moisture content was the varying predictor variable, it was varied from its low value to its high value, density was held constant at its high value, cutting velocity constant at its low value, and depth-of-cut at its high value.

The third case, the low-force case, again consisted of varying one of the predictor variables between the same low and high values and holding the other three predictor variables constant. However, they were held constant at values that would decrease the response variables. Returning to the moisture content example, density would be held constant at its low value, cutting velocity at its high value, and depth-of-cut at its low value. To summarize, each case consists of varying one predictor variable while the others held at their mean value (mid-force case), maximum-force value (high-force case), or minimum-force value (low-force case).

Results are given in Table 4 for the effects of all three cases. For each case and variable combination, three parameters were calculated: the force mean ($\overline{F}$, the force magnitude corresponding to the mean value of the varying predictor variable), the force slope ($\Delta F/\Delta PV$**,** the change in force magnitude per unit change in the varying predictor variable), and the force change ($\Delta F/F$, the change in force magnitude with respect to the varying predictor variable divided by the force magnitude calculated at the low value of the varying predictor variable and expressed as a percentage).

Table 4. Effect of Changing Predictor Variable Magnitude

		High-Force			Mid-Force			Low-Force		
		$\overline{F}$ [N]	$\frac{\Delta F}{\Delta PV}$	$\frac{\Delta F}{F}\%$	$\overline{F}$ [N]	$\frac{\Delta F}{\Delta PV}$	$\frac{\Delta F}{F}\%$	$\overline{F}$ [N]	$\frac{\Delta F}{\Delta PV}$	$\frac{\Delta F}{F}\%$
MC	F_{CH}	204.4	−4.78	−12.5%	106.3	−2.29	−11.6%	23.2	0.20	5.1%
	F_C	171.4	−4.12	−12.9%	85.3	−2.12	−13.3%	10.3	−0.12	−6.2%
	F_F	103.8	−3.64	−18.3%	41.4	−1.67	−20.7%	0.1	0.36	231.1%
ρ	F_{CH}	210.6	0.25	7.0%	106.3	0.16	8.8%	25.6	0.06	15.1%
	F_C	176.7	0.23	7.7%	85.3	0.14	9.9%	11.5	0.05	29.9%
	F_F	107.1	0.25	14.4%	41.4	0.14	21.5%	1.8	0.03	162.0%
V_C	F_{CH}	215.9	−0.62	−1.6%	106.3	−0.62	−3.3%	25.6	−0.62	−13.0%
	F_C	181.4	−0.65	−2.0%	85.3	−0.65	−4.3%	11.9	−0.65	−27.2%
	F_F	113.3	−0.33	−1.7%	41.4	−0.33	−4.5%	2.0	−0.33	−65.2%
δ	F_{CH}	123.8	313.1	630%	111.1	280.5	628%	98.2	247.9	625%
	F_C	100.3	276.5	955%	88.3	248.9	1092%	76.4	221.3	1329%
	F_F	58.5	185.9	4047%	48.8	156.3	4985%	39.1	126.8	7547%

From the data in Table 4, several trends can be identified. For all cases and response variables, chain force has the largest magnitude and feed force the least, as shown by the force-mean parameter. For example, consider the high-force case of moisture content. Listed vertically, chain force exhibited the greatest magnitude of 204.4 N, cutting force a magnitude of 171.4 N, and feed force the least at 103.8 N. Interaction effects were shown by changes in the magnitude of the force-slope parameter. For example, consider cutting velocity. Reading horizontally across the table, the force-slope parameter has the same values of -0.62 for chain force, -0.65 for cutting force, and -0.33 for feed force for the high-force, mid-force, and low-force cases, indicating that no interaction exists. Additionally, the magnitude of the slope parameter was small for all forces and cases, indicating that overall, cutting velocity had a small effect on the response variables compared with the other predictor variables in the model. The moisture-content-depth-of-cut interaction and density-depth-of-cut interactions were evident from the changing values of the force slope parameter. Figure 10 graphically displays these interactions through differing slopes of the regression trend line for the high-force, mid-force, and low-force cases of chain force. If no interaction existed, the slope would not change with each force case. Similar trends were observed for cutting force and feed force. The force change parameter showed that although force slope became small at the low-force condition, the change in force relative to its magnitude can be large.

Of particular interest is the moisture-content-depth-of-cut interaction. When moisture content is the varying predictor variable (*i.e.*, the rows of Table 4 labeled MC), the effect of the moisture-content-depth-of-cut interaction is shown by the force-slope parameter. For all three forces, this parameter had its greatest magnitude in the high-force case. The high force case corresponds to depth-of-cut at its maximum value. Thus, moisture content had its greatest effect on the three forces at high depths-of-cut. As the case changed from high-force to mid-force to low-force, the depth-of-cut decreased. The moisture-content-depth-of-cut interaction caused the force slope parameter to decrease in magnitude and become increasingly positive and actually become positive in the low-force case for chain force (0.20) and feed force (0.36). Thus, for all but the smallest depth-of-cut values,

all three forces decreased with increasing moisture content, with the effect being greatest at high depths-of-cut (the high-force case). However, at low depths-of-cut, the trend reversed and chain force and feed force increased with increasing moisture content. This trend is shown graphically in Fig. 10(a), where the slope of the regression trend line changes from negative in the high-force case to slightly positive in the low-force case.

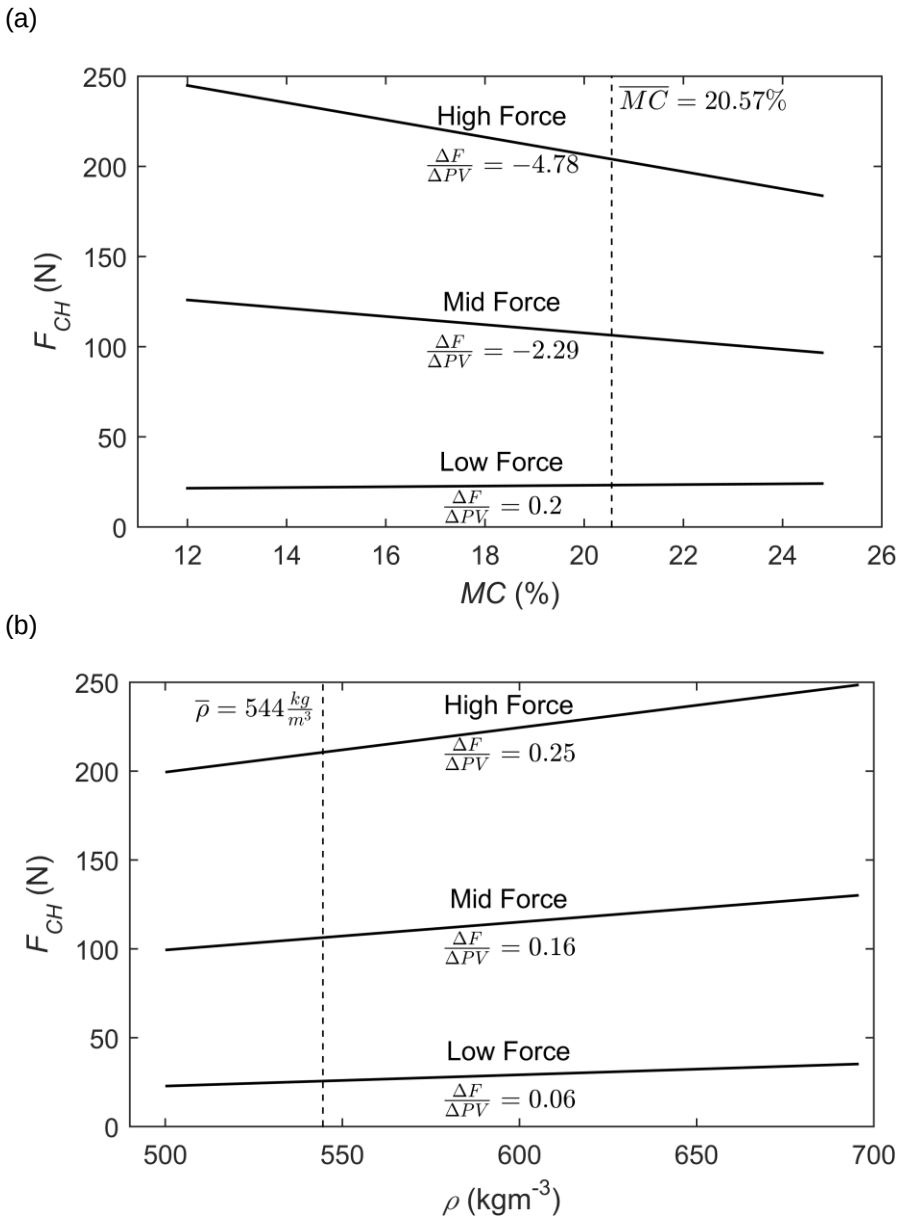

Fig. 10. Interaction of (a) moisture content and (b) density with depth of cut on affecting chain force magnitude for the three force cases.

This trend in the magnitude of effects with depth-of-cut has a basis in prior work. The cutting force model developed by Atkins (2009) provides a theoretical foundation for the existence of interactions in which physical properties have a reduced influence on cutting forces at low depths-of-cut. The model proposed by Atkins is the following,

$$F_C = \left(\frac{kw\gamma}{Q} + \frac{R}{Q}\right)\delta + \frac{Rw}{Q} \quad (4)$$

where k is the shear yield strength, w is the kerf width, γ is the shear yield strain along the primary shear band, Q is a function of friction coefficients and tool geometry, and R is the specific work of surface separation. Material-dependent parameters in the model are k and R. As can be seen, the first term in parentheses multiplying δ was controlled by material properties. Since moisture content and density can be correlated with mechanical properties (Kretschmann 2010), the first term in the Atkins cutting model is captured by the interaction terms of the regression model. Furthermore, Chuchala *et al*. (2014) provides experimental data clearly showing that different trend line slopes are required to explain changes in cutting forces due to density at two different depth-of-cut levels. These findings support the inclusion and significance of an interaction term between physical properties and depth-of-cut in the present linear regression model.

Depth-of-cut had a significant effect on all response variables. Due to the density-depth-of-cut interaction, the greatest change in force slope occurred in the high-force case; however, unlike the effect of moisture content, this effect was uniformly positive. That is, in all cases, increased density resulted in increased cutting force, with the greatest effect at high depths-of-cut. Over the range of values of predictor variables included in the study, depth-of-cut had the greatest effect on forces. Relative effects tended to be greatest for the low-force case but were in general very large. Increasing depth-of-cut consistently and significantly increased all forces.

Cutting Efficiency

Cutting efficiency is a measure of the amount of cutting performed by a unit input of energy. It is a useful metric because it accounts for energetic losses that are independent of time. A high efficiency corresponds to a large amount of cutting from a small input of energy, and a low efficiency corresponds to the reverse. Denoted by η, cutting efficiency can be calculated as,

$$\eta = 1000\frac{V_F L}{F_{CH} V_C}, \quad (5)$$

where V_F, F_{CH}, and V_C are as previously defined, and L is the length of cut (here, the length of cut is equal to the 90 mm width of the workpieces). Equivalently, substituting $V_F/V_C = \delta/PS$, cutting efficiency can also be calculated as:

$$\eta = 1000\frac{\delta L}{F_{CH} PS}. \quad (6)$$

Chain force, rather than cutting force, is used in the calculation of cutting efficiency so that losses in the drive train are included. Figure 11 shows cutting efficiency, chain force, cutting force, and feed force trend lines as a function of depth-of-cut, all calculated using the regression model. To capture the influence of the other predictor variables in the regression model, cutting efficiency is shown as a range of values from the high-force condition (lower solid line), mid-force condition (dashed line), and low-force condition (upper solid line). Chain force, cutting force, and feed force are all calculated at mid-force-conditions. Cutting efficiency reaches a maximum value at a depth-of-cut equal to the overload value.

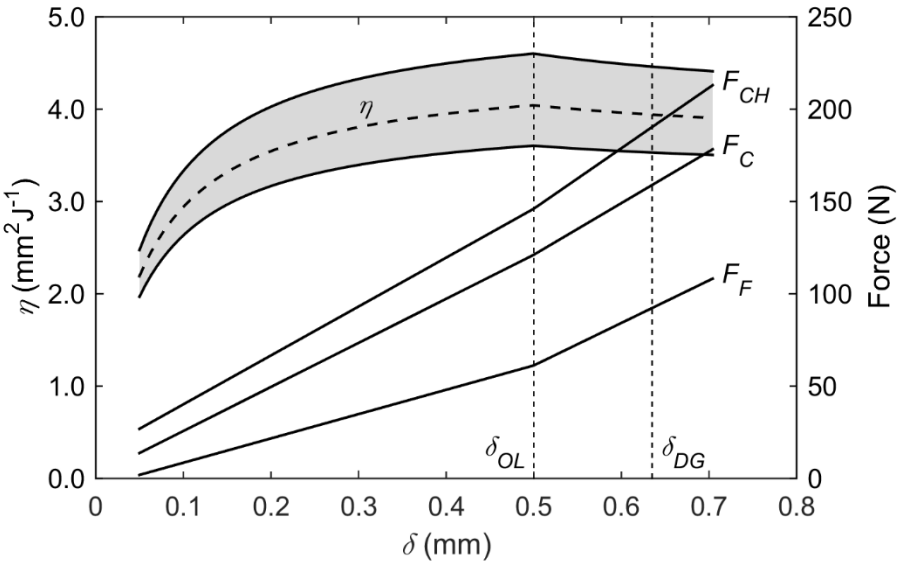

Fig. 11. Cutting forces and cutting efficiency plotted *versus* depth-of-cut with the overload point and depth gauge setting indicated

Given the significance of the overload value of depth-of-cut, it is worthwhile to consider what causes this and the corresponding bilinear force behavior to occur. Possible causes are the depth gauge setting and the effect of chip removal. Due to link rotation during cutting (Stacke 1989), the depth gauge may be pushed into the kerf bottom at depth-of-cut values less than the chain's actual depth gauge setting. Pushing the depth gauge into the kerf bottom results in increased cutting forces, both through indentation (feed force) and friction (cutting force and chain force). Also, chip removal could be a contributor due to the increase in chip size with depth-of-cut and the limited volume available in the kerf. When the available volume becomes overfilled, forces could increase at a larger rate, causing bilinear behavior.

Beneficial future work could consist of extending the range of the predictor variables included in the study. The range of moisture content and density included in the study depended on the variation in the chosen Douglas-fir dimensional timbers. While this variation was sufficient to show meaningful trends, obtaining specimens with a wider range of moisture content and density would likely show interesting results. The inclusion of greater cutting velocities, as previously discussed, would allow the exploration of a possible optimum efficiency value at high velocities. Depth-of-cut could be further explored by varying depth gauge setting and cutter tooth geometry to investigate the causes of the overload depth-of-cut phenomena.

CONCLUSIONS

1. The change in rate of increase of cutting forces with depth-of-cut can be accurately represented by a bilinear model.
2. An optimum exists for saw-chain cutting efficiency, and it occurs at a depth-of-cut equal to the newly-termed overload value.

3. Through the inclusion of workpiece moisture content and density, an accurate regression model can be created for the prediction of saw-chain cutting forces that accounts for the inherent heterogeneity of wood mechanical properties.
4. Using this model, trends and interactions can be identified. It was shown that these trends and interactions, while newly presented for saw chains, are consistent with prior work in other types of cutting.
5. Over the range of workpiece moisture content measured in the study (12.0% to 24.8%), increasing moisture content was found to cause chain force, cutting force, and feed force to increase for all but the smallest depth-of-cut, with the effect being greatest at high depths-of-cut. At the smallest depth-of-cut, increasing moisture content caused chain force and feed force to increase.
6. Workpiece density, over the range measured (500 kg/m^3 to 695 kg/m^3), consistently caused all forces to increase, with the greatest effect seen with high depths-of-cut.
7. Cutting velocity, varying from 3.81 m/s to 9.525 m/s, was not found to have a large effect on any of the cutting forces.
8. Increases in depth-of-cut were found to cause chain force, cutting force, and feed force to greatly increase. This increase was found to have a bilinear behavior, with the effect of depth-of-cut being greater above a specific depth-of-cut denoted the overload depth-of-cut. In general, these trends agree with the prior research in orthogonal cutting and rigid-cutter sawing described previously in this paper.
9. For the typical saw chain, guide bar, and testing conditions of this study, optimum efficiency occurred at a feed force of nearly 60 N. This is approximately equal to the total weight of a typical battery-powered chainsaw, providing a convenient guideline for users.
10. For chainsaw manufacturers, the near independence of cutting forces with cutting velocity means that attaining optimal cutting efficiency depends primarily on the ability of the motor to supply sufficient driving torque, not power. Designing chainsaws to operate at optimum efficiency tends to extend battery life, an important consideration for cordless tools.

REFERENCES CITED

Atkins, A. (2009). "Sawing, chisels, and files," in: *The Science and Engineering of Cutting*, Atkins, A. (ed.), Butterworth-Heinemann, Oxford. DOI: 10.1016/B978-0-7506-8531-3.00007-9

Bucar, B., and Bucar, D. G. (2002). "The influence of the specific cutting force and cross-sectional geometry of a chip on the cutting force in the process of circular rip-sawing," *European Journal of Wood and Wood Products* 60(2), 146-151. DOI: 10.1007/s00107-002-0281-5

Chuchala, D., Orlowski, K. A., Sandak, A., Sandak, J., Pauliny, D., and Baranski, J. (2014). "The effect of wood provenance and density on cutting forces while sawing scots pine," *BioResources* 9(3), 5349-5361. DOI: 10.15376/biores.9.3.5349-5361

Coutermarsh, B. A. (1989). *Factors Affecting Rates of Ice Cutting with a Chain Saw*, US Army Corps of Engineers, Cold Regions Research and Engineering Laboratory, Hanover, NH.

Cristovao, L., Broman, O., Gronlund, A., Ekevad, M., and Sitoe, R. (2012). "Main cutting force models for two species of tropical wood," *Wood Material Science and Engineering* 7(3), 143-149. DOI: 10.1080/17480272.2012.662996

Franz, N. C. (1958). *An Analysis of the Wood-cutting Process*, University of Michigan Press, Ann Arbor, MI.

Gronlund, A. (1988). "Measuring and modelling of cutting forces," *Proceedings of the 9th International Wood Machining Seminar*, University of California Forest Products Laboratory, Richmond, CA, 342-350.

Heinzelmann, G., Liebhard, G., and Rosskamp, H. (2011). "Energy efficient drive train for a high-performance battery chain saw," *Proceedings of the 1st International Electric Drives Production Conference*, Nuremburg, DE, 101-106. DOI: 10.1109/EDPC.2011.6085558

Kivimaa, E. (1950). "Cutting force in woodworking," VTT, Helsinki.

Koch, P. (1964). *Wood Machining Processes*, Ronald Press Co., New York.

Kretschmann, D. E. (2010). "Mechanical properties of wood," in: *Wood Handbook, Wood as an Engineering Material*, USDA Forest Products Laboratory, Madison, WI.

McMillin, C.W., and Lubkin, J. L. (1959). "Circular sawing experiments on a radial arm saw," *Forest Products Journal* 9(10), 361-367.

McKenzie, W. M. (1955). "The performance of gouge type power saw chains," *Australian Timber Journal* 21(10), 938-954, 995.

McKenzie, W. M. (1961). *Fundamental Analysis of the Wood-cutting Process*, PhD Dissertation, University of Michigan, Ann Arbor, MI.

Naylor, A., Hackney, P., Perera, N., and Clahr, E. (2012). "A predictive model for the cutting force in wood machining developed using mechanical properties," *BioResources* 7(3), 2883-2894. DOI: 10.15376/biores.7.3.2883-2

Oehrli, J. W. (1960). "Dynamometer tests on cutting action of chain-saw teeth," *Forest Products Journal* 10(1), 4-7.

Orlowski, K. A., Ochrymiuk, T., Atkins, A., and Chuchala, D. (2013). "Application of fracture mechanics for energetic effects while wood sawing," *Wood Science and Technology* 47(5), 949-963. DOI: 10.1007/s00226-013-0551-x

Reynolds, D. D., Soedel, W., and Eckelman, C. (1970). "Cutting characteristics and power requirements of chain saws," *Forest Products Journal* 20(10), 28-34.

Ryan, T. P. (2009). *Modern Regression Methods*, John Wiley and Sons, Hoboken, NJ.

Stacke, L. E. (1989). *Cutting Action of Saw Chains*, Ph.D. Dissertation, Chalmers University of Technology, Gothenburg, Sweden.

Wyeth, D. J., Goli, G., and Atkins, A. (2009). "Fracture toughness, chip types, and the mechanics of cutting wood," *Holzforschung* 63(2), 168-180. DOI: 10.1515/HF.2009.017

Article submitted: April 20, 2015; Peer review completed: July 6, 2015; Revised version received: August 22, 2015; Accepted: August 23, 2015; Published: September 9, 2015.
DOI: 10.15376/biores.10.4.7273-7291